Available online at www.sciencedirect.com
SCIENCE DIRECT®
Journal of Solid State Chemistry 177 (2004) 2456–2463
JOURNAL OF SOLID STATE CHEMISTRY
http://elsevier.com/locate/jssc

Characterization of brookite and a new corundum-like titania phase synthesized under hydrothermal conditions

X. Bokhimi[a,*,1] and F. Pedraza[b]

[a] Institute of Physics, The National University of Mexico (UNAM), A.P. 20-364, 01000 México D.F., Mexico
[b] Molecular Engineering Program, Instituto Mexicano del Petróleo, Eje Central L. Cárdenas 152, A.P. 14-805, 07730 México D.F., Mexico

Received 3 October 2003; received in revised form 16 January 2004; accepted 7 April 2004

Abstract

Brookite rich samples were synthesized under hydrothermal conditions by using $TiCl_3$ as precursor. They also contained a new titanium oxide phase that has the same crystalline structure as Ti_2O_3, and is stable after annealing in air. Samples were characterized with X-ray powder diffraction, transmission electron microscopy and thermogravimetry. Crystalline phases were refined by using the Rietveld method, from which phase concentrations and atomic bond lengths were obtained as a function of sample annealing temperature. Samples contained brookite, anatase, rutile and the new corundum-like phase: Brookite's concentration was larger than 50 wt%, while the one of the corundum-like phase reached 20(6) wt%. The local symmetry and the atomic bond lengths of these two phases depended on the crystallite size; for both, there is a correlation between the evolution of the atomic bond lengths with temperature and their transformation into another phase. The hydrothermal conditions stabilized brookite, anatase, and the corundum-like phase at high temperature: This last phase was stable in air, even at 900°C.

Keywords: Brookite rich samples; Corundum-like titania phase synthesis; Brookite's stability; $TiCl_3$ as titania precursor; Synthesis under hydrothermal conditions

1. Introduction

Titania is one of the most interesting materials used nowadays in high technology [1–4]. It has many polymorphs [5], from which anatase brookite and rutile are the most stable [6], and can be synthesized at low temperature [7–9]. Because single-phase samples of anatase [10] and rutile [11] are prepared easily, they have been widely characterized; therefore, their physical and chemical properties are well known [12–14].

During the synthesis of anatase, frequently brookite appears as a secondary minority phase [6]. A precise explanation for its appearance, however, has not been given, which hinders the possibility of sintering samples with only brookite, by just varying the synthesis parameters. Recently, brookite-rich samples were prepared at low temperature [9,15]. In one case by thermolysis of strongly acidic solutions [9], and in the other by hydrothermal treatment of basic solutions [15]. In the present work, we obtained brookite from an acidic solution treated under hydrothermal conditions. Initially, this treatment was not for getting brookite, but to extend our previous study of the rutile obtained by annealing this acidic solution at 90°C [16]. The initial goal of the hydrothermal treatment was to control rutile's crystallite size, in a similar way as it is done during the synthesis of boehmite [17,18].

It is important to notice that in many applications of titania [19], the interpretation of the results is incorrect, because the concentration of each polymorph is not considered. In the case that the concentration of each titania phase is known and brookite is one of them, an additional problem exists: The properties of pure brookite are scarcely known, because of the difficulty of preparing samples with only this phase. This makes evident the urgency of working more on the synthesis of single-phase brookite samples to characterize this phase.

*Corresponding author. Fax: +52-562-250-08.
E-mail address: bokhimi@fisica.unam.mx (X. Bokhimi).
[1] Advisor at Instituto Mexicano del Petróleo.

0022-4596/$ - see front matter © 2004 Elsevier Inc. All rights reserved.
doi:10.1016/j.jssc.2004.04.021

This problem has been solved by nature because brookite is found in minerals forming large crystals [20], from which its crystalline structure was determined [21]. The corresponding synthesis conditions have not been discovered until now, but the results suggest, that a hydrothermal environment is important [22].

In the recent papers about brookite synthesis at low temperature [9,15], from the X-ray powder diffraction analysis authors claim that samples contain only brookite. For the interpretation of the diffraction patterns, however, they have not taken into account the fact that the main diffraction peaks of brookite and anatase overlap. So, the apparently pure brookite samples can be a mixture of anatase and brookite. The only way to prove that samples are single phase is to run their X-ray powder diffraction patterns with a good statistic to refine the crystalline structure of brookite in order to demonstrate that the modeling of only this phase is enough to reproduce the experimental diffraction pattern.

In the present work, we characterize the brookite synthesized under hydrothermal conditions from an acidic solution of $TiCl_3$. The fresh samples appeared to be almost single phase containing brookite with a small amount of rutile. The refinement of the crystalline structure of brookite by using the Rietveld method, however, showed that brookite was the main phase, but that the sample also contained anatase. Brookite and anatase phases were stable at high temperatures: Their transformation into rutile occurred above 800°C.

When samples were annealed in air, it appeared a new crystalline phase, which was modeled with the crystalline structure of Ti_2O_3 and the same chemical composition. The new phase, however, did not oxidize when it was annealed in air above 400°C, in contrast to Ti_2O_3, which transforms into rutile phase.

2. Experimental

2.1. Sample preparation

Five grams of $TiCl_3$ (Aldrich, 99.999%) were dissolved in 300 mL of bi-distilled water; the pH of this solution was set to 1 with HCl. When this solution is annealed at 90°C, samples contains only rutile [16]. In order to extend the studies of rutile, we tried to control its crystallite size by annealing the solution under hydrothermal conditions. The acidic solution was put into the vessel of the autoclave, filling 3/4 of its capacity, and annealed at 200°C for 3 days; the generated pressure was of 20.4 Atm. Eventually the annealed solution was cooled to room temperature, filtered, and dried in air at 100°C for 12 h (fresh sample). To our surprise, after the above annealing the fresh sample contained not only rutile, but also anatase and brookite, which was the main phase. The dried powder was additionally annealed for 12 h in air at 200°C, 300°C, 400°C, 500°C, 600°C, 700°C, 800°C, 900°C, 1000°C and 1070°C.

2.2. Characterization

2.2.1. X-ray powder diffraction

The X-ray diffraction pattern of the sample packed in a glass holder was recorded at room temperature with CuK_α radiation in a Bruker Advance D-8 diffractometer that had a $\theta-\theta$ configuration and a graphite monochromator in the secondary beam. Diffraction intensity was measured between 15° and 135°, with a 2θ step of 0.02° for 6.0 s per point. Sample was 1.5 mm thick, which was enough to hinder any contribution from the sample holder to the diffraction patterns. Crystalline structures were refined with the Rietveld technique by using FULLPROF98 code [23]; peak profiles modeled with pseudo-Voigt functions [24] contained average crystallite size and microstrain as two of the characteristic parameters to be refined [25]; the reliability of these parameters is discussed in detail elsewhere [26]. The effect of the microstrain was included in the Gaussian part of the function, while the corresponding effect of the size was included in the Lorentzian one. The standard deviations, modified by taking into account serial correlations [27], of the refined parameters are not estimates of the probable error in the analysis as a whole, but only of the minimum possible probable errors based on their normal distribution [28].

Fifty three were the maximum number of refined variables. For brookite, they included the scale factor, all atom fractional coordinates, isotropic atomic displacements, atom occupancies, lattice parameters, microstrain, and isotropic crystallite size; for anatase, the variables included the only atom fractional coordinate that can be refined, the z coordinate of oxygen atom, as well as the scale factor, isotropic atomic displacements, titanium atom occupancy, lattice parameters, microstrain and isotropic crystallite size. For rutile, the refined variables included the scale factor, the x and y atom fractional coordinates of oxygen atom, isotropic atomic displacements, titanium occupancy, lattice parameters, microstrain and the anisotropic crystallite size with a needle-like model. For the corundum-like titania (CLT) phase, the refined parameters included the scale factor, the variable atom fractional coordinates Ti_z and O_x, isotropic atomic displacements, titanium occupancy, lattice parameters, microstrain and the isotropic crystallite size.

2.2.2. Thermoanalysis

The weight loss and the temperatures associated to phase transformations were determined by thermogravimetry with a Perkin-Elmer TG-7 apparatus; samples

were heated from room temperature up to 1000°C at 10°C/min.

2.2.3. Transmission electron microscopy (TEM)

Samples were milled to get small grain size and dispersed in ethanol, then transferred to a copper grid covered with formvar resin (polyvinyl acetal). They were observed at 200,000 X with 100 KV in a Jeol 100CX transmission electron microscope that had high-resolution pole pieces. In order to have a correlation with X-ray powder diffraction patterns, the analysis was performed in the fresh sample and in those annealed at 300°C, 500°C, 700°C and 900°C.

3. Results and discussion

Samples contained four different crystalline phases: Brookite, anatase, rutile and one phase with the same crystalline structure as the Ti_2O_3 phase, but in contrast to Ti_2O_3, it did not oxidize when it was annealed in air at high temperatures; this phase was named CLT. In order to have a good identification of this phase and to find the origin of its stabilization, it is necessary to synthesize single-phase samples containing only it. The CLT phase concentrations, determined by refining the crystalline structures with the Rietveld method, depended on the sample annealing temperature (Fig. 1 and Table 1).

In order to perform the refinement, the crystalline structure of brookite was modeled with an orthorhombic unit cell that had the symmetry given by space group

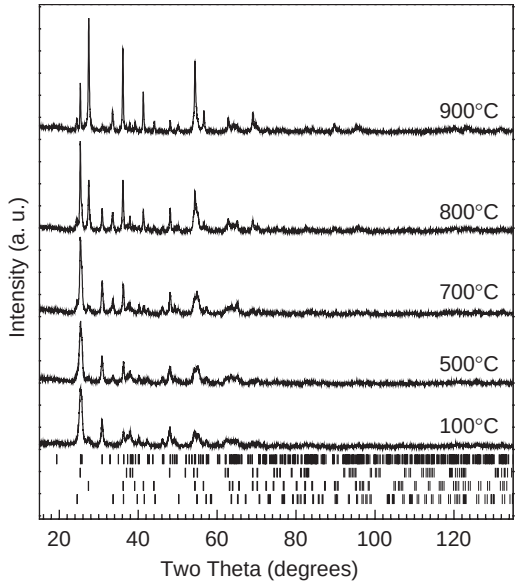

Fig. 1. X-ray powder diffraction patterns for the different sample annealing temperatures. From top to down, the first tick marks correspond to brookite, the second ones to anatase, the next ones to rutile, and the last ones to CLT phase.

Table 1
Phase concentrations in wt% as a function of sample annealing temperature

T (°C)	Brookite	Anatase	Rutile	CLT
100	61(4)	33(4)	6(1)	—
200	63(9)	31(7)	6(2)	—
300	64(8)	30(6)	6(2)	—
400	60(8)	29(6)	6(4)	5(4)
500	57(7)	28(6)	5(4)	10(4)
600	56(10)	24(5)	5(8)	15(5)
700	53(8)	22(5)	7(5)	18(5)
800	27(6)	22(3)	31(6)	20(6)
900	6(3)	12(3)	62(6)	20(6)

Table 2
Brookite, space group *Pbca* (61) Atom coordinates in unit cell

Atom	Site	x	y	Z
Ti	8*c*	Ti_x	Ti_y	Ti_z
O1	8*c*	$O1_x$	$O1_y$	$O1_z$
O2	8*c*	$O2_x$	$O2_y$	$O2_z$

The starting values for these coordinates [6] were: $Ti_x = 0.127$, $Ti_y = 0.113$ $Ti_z = 0.873$; $O1_x = 0.010$, $O1_y = 0.155$, $O1_z = 0.180$; $O2_x = 0.230$, $O2_y = 0.105$, $O2_z = 0.465$.

Table 3
CLT, space group *R*-3*c* (167) atom coordinates in unit cell

Atom	Site	x	y	z
Ti	12*c*	0.0	0.0	Ti_z
O	18*e*	O_x	0.0	0.25

The initial Ti_z and O_x coordinates [29] were 0.3464 and 0.311, respectively.

Pbca and the atom positions given in Table 2. The crystalline structure of anatase was modeled with a tetragonal unit cell having the symmetry described by space group $I4_1/amd$ and the atom positions reported elsewhere [6]. The structure of rutile was modeled with a tetragonal unit cell whose symmetry is given by space group $P4_2/mnm$ and the atom positions described elsewhere [6]. The crystalline structure of the CLT phase was modeled with the same crystalline structure as Ti_2O_3 [29]: It corresponds to a hexagonal unit cell that has the symmetry given by space group *R*-3*c* and atoms in the positions reported in Table 3. To have an idea of the goodness of the refinement Fig. 2 shows the Rietveld refinement plot of the sample annealed at 500°C.

The initial model for the refinement included only brookite and rutile phases, but it gave rise to a poor fitting of the experimental diffraction pattern; this, however, was improved when anatase was included in the model.

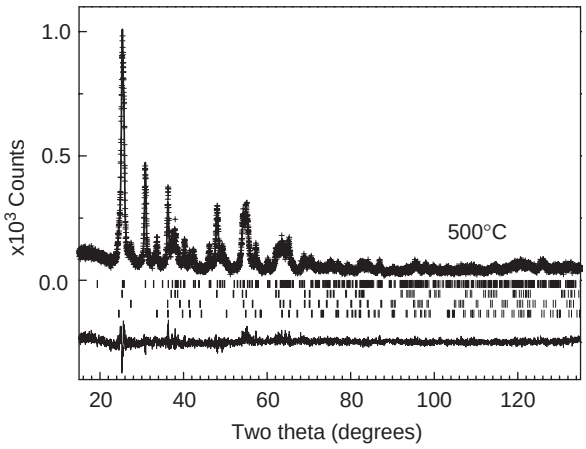

Fig. 2. Rietveld refinement plot of the sample annealed at 500°C. From top to down, the first tick marks correspond to brookite ($R_B = 0.082$), the second ones to anatase ($R_B = 0.071$), the next ones to rutile ($R_B = 0.098$), and the last ones to CLT phase ($R_B = 0.106$).

Table 4
Average crystallite size in nm as a function of sample annealing temperature

T (°C)	Brookite	Anatase	Rutile	CLT
100	21.6(7)	12.9(6)	20(9)	—
200	27(2)	15(2)	23(20)	—
300	25(1)	15 (1)	20(10)	—
400	24(1)	16(2)	25(18)	21(8)
500	26(2)	16(2)	20(17)	26(6)
600	26(2)	20(3)	17(13)	26(5)
700	33(3)	26(3)	20(13)	33(5)
800	38(6)	43(6)	29(9)	43(9)
900	27(9)	87(15)	36(9)	60(15)

When the annealing temperature of the sample was lower than 400°C, the only observed crystalline phases were brookite (the main phase) anatase and rutile (Table 1), in concentrations that were almost independent of annealing temperature. In this temperature range, the CLT phase was probably present as an amorphous phase or as crystallites smaller than 2.0 nm in diameter.

The crystalline CLT phase appeared in the sample when it was annealed at 400°C (Table 1). At this temperature, the Rietveld analysis showed that only 5(4) wt% of the sample corresponded to this phase with an average crystallite size of 21.6(7) nm (Table 4). This size increased significantly only after the sample was annealed at 700°C.

The sudden appearance of CLT phase in the diffraction pattern when the sample was annealed at 400°C suggests the presence of this phase even in the fresh sample, although it was not observed in the X-ray powder diffraction pattern. Therefore, we searched for it in all samples by using transmission electron microscopy (Fig. 3).

From the micrographs it was observed that the fresh sample (Fig. 3A) comprised a mixture of large brookite crystallites, which were slabs about 25 nm width and 75 nm length, with smaller slabs corresponding to anatase, and needles corresponding to rutile. This last phase has been well identified with this technique in pure rutile samples [16]. Together with these crystallites there were regions of quasi-amorphous material, which were still present in the sample annealed at 500°C (Fig. 3B). In this figure it was observed that this quasi-amorphous material was not dispersed at random: it formed coherent regions (larger than 50 nm), which were probably the precursors of the CLT crystals when the sample was annealed at higher temperatures (Table 4).

The thermogravimetric analysis (Fig. 4A) shows that samples had a weight loss of 2.2 wt% between 370°C and 800°C, which correlates well with the temperature region where the CLT phase crystallized. The corresponding lost material in this temperature range was the one that maintained the small CLT crystallites together (Fig. 3B) avoiding their sintering. With the actual samples it is difficult to analyze in detail this phase; therefore, we are working on obtaining samples with a larger concentration of the CLT phase, before speculating any possibly explanation for this phenomenon. This weight loss could be produced by hydroxyls strongly bonded to the surface of CLT crystallites. For comparison, Fig. 4B gives the TG curve of the sample of pure rutile obtained with the solution used in the present work for the synthesis but without the hydrothermal treatment [16]. This curve does not have the weight losses observed for the hydrothermally annealed sample, it has only the ones corresponding to the dehydration and dehydroxilation of the sample [16].

The lattice parameters of the CLT phase grew as crystallite size was increased (Table 5); the lattice parameter a, however, was considerably shorter than the one of the Ti_2O_3 phase [29]. This, together with the titanium deficiency in the crystalline structure (Table 5) produced by the high valence (4+) of the titanium atoms, suggested by the absence of oxidation of the phase when it is annealed in air, gave rise to a distortion of the characteristic octahedron of the phase.

This octahedron and its interaction with the next neighboring octahedra (Fig. 5) describe the local symmetry associated to this lattice. The representative octahedron is well described with six different atomic bond lengths and the angle ϕ formed by the atomic bond lengths T_1 and T_2 (Tables 6 and 7); the lattice is built by the arrangement of these octahedra. To any octahedron there is associated another octahedron sharing the face defined by the three atomic bond lengths T_5, which are perpendicular to [001] direction; the Ti–Ti interaction between these octahedra, represented by the atomic bond length T_7, is strong (Table 7), but weaker than in large crystallites of the Ti_2O_3 phase

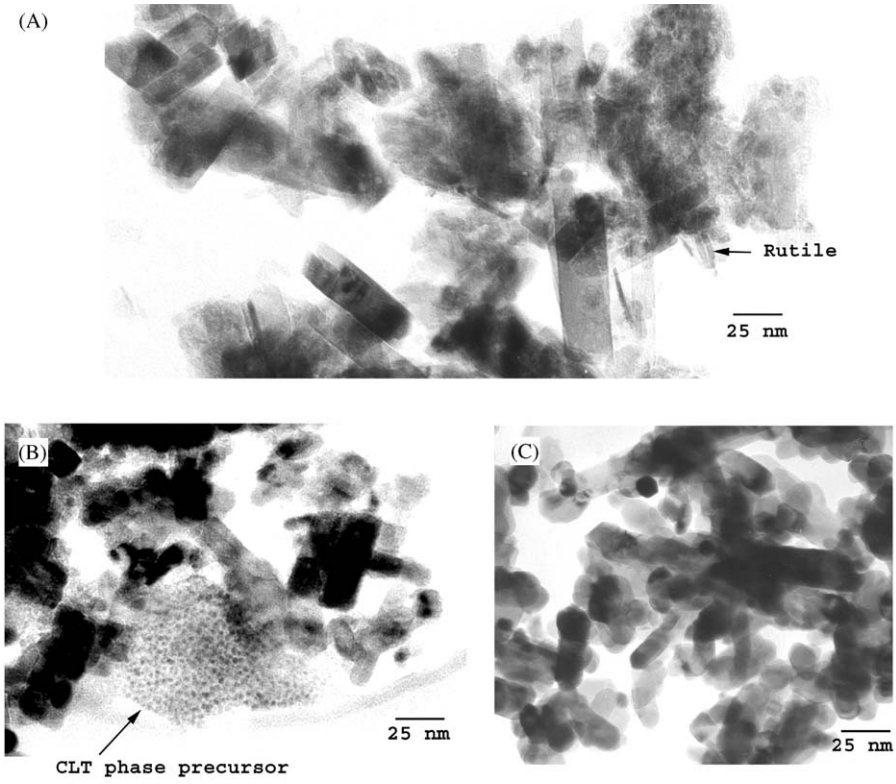

Fig. 3. TEM images of the samples after their annealing: (A) at 100°C, (B) at 500°C, and (C) at 700°C.

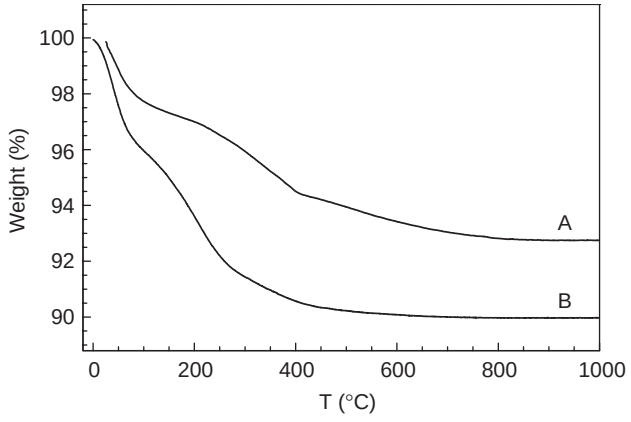

Fig. 4. (A) Thermogravimetric curve in air of the fresh sample as a function of temperature. (B) The corresponding thermogravimetric curve of the sample prepared without hydrothermal treatment, which contains only rutile.

[29]. Here the atomic bond length is 0.2582(2) nm while in the CLT phase the corresponding length is 0.2697(6) for the largest crystallites. Additional to the above face sharing octahedron, there are three more octahedra sharing each one of the three atomic bond lengths T_3 (represented by thick lines in the figure). These edge-sharing octahedra lie along a–b plane, and give rise to the Ti–Ti interaction T_8, which is weaker than the one corresponding to the face sharing octahedron (Table 7).

Table 5
CLT: Lattice parameters and atom coordinates Ti_z and O_x and titanium occupancy as a function of sample annealing temperature

T (°C)	a (nm)	c (nm)	Ti_z	O_x	Ti occupancy
400	0.4957(6)	1.357(2)	0.344(2)	0.33(2)	0.87(14)
500	0.4955(2)	1.3604(9)	0.345(1)	0.325(7)	0.84(9)
600	0.4958(2)	1.359(1)	0.346(1)	0.323(8)	0.90(15)
700	0.4964(2)	1.3605(8)	0.3476(8)	0.320(5)	0.90(15)
800	0.4972(2)	1.3622(6)	0.3481(9)	0.325(6)	0.90(9)
900	0.4977(2)	1.3633(6)	0.349(1)	0.328(6)	0.87(9)

In contrast to the Ti–Ti interaction associated to the face sharing octahedra, the interaction between edge sharing octahedra in the CLT phase is stronger than in Ti_2O_3 phase [29]. The associated atomic bond length to this last phase is 0.2994(1) nm while the largest value in CTT phase was 0.2904(2) nm.

The interaction associated to the atomic bond length T_1 in the CLT phase was significantly stronger than the one corresponding to Ti_2O_3 phase [29]. In this Ti^{3+} phase the atomic bond length is 0.2024(1) nm while in the CTT phase the largest value was 0.1937(2) nm.

The O–O interactions associated with the T_3 and T_5 atomic bond lengths, which maintain together the octahedra, became weaker as the annealing temperature was increased. This explains the transformation of this

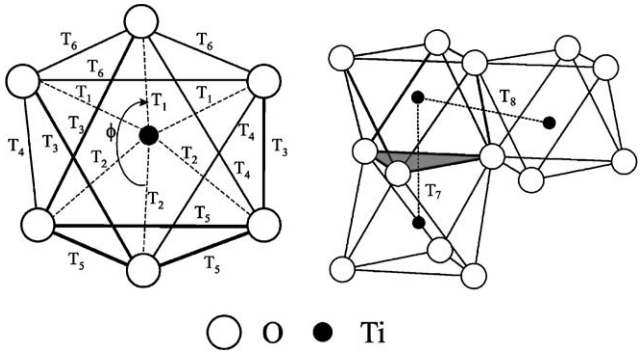

Fig. 5. Representative octahedron of CLT phase with identification of the different atomic bond lengths associated to it. The shared edges T_3 are enhanced, as well as the edges T_5 that define the face of the octahedron that is shared with one of its neighboring octahedra. The figure gives also details of how octahedra are shared, and the corresponding Ti–Ti bonds, T_7 and T_8.

Table 6
CLT: Atomic bond lengths (in nm) associated to the representative octahedron as a function of sample annealing temperature

T (°C)	T_1	T_2	T_3	T_4	T_5	T_6
400	0.1931(2)	0.2074(2)	0.2791(4)	0.2806(4)	0.2833(1)	0.28763(8)
500	0.1937(2)	0.2064(2)	0.2782(4)	0.2818(4)	0.2789(1)	0.28972(8)
600	0.1931(2)	0.2069(2)	0.2776(5)	0.2820(5)	0.2774(2)	0.2908(1)
700	0.1932(2)	0.2070(2)	0.2771(5)	0.2827(5)	0.2751(2)	0.2925(1)
800	0.1921(3)	0.2099(3)	0.2788(6)	0.2823(6)	0.2799(2)	0.2907(1)
900	0.1910(3)	0.2117(3)	0.2798(6)	0.2821(6)	0.2827(2)	0.2896(1)

Table 7
CLT angle ϕ between opposite atomic bond lengths, and the Ti–Ti atomic bond lengths (in nm) between neighboring octahedra, as a function of sample annealing temperature

T (°C)	ϕ (deg)	T_7	T_8
400	172.7(1)	0.2551(4)	0.2877(1)
500	171.5(1)	0.2582(4)	0.2878(1)
600	170.3(2)	0.2621(5)	0.2884(2)
700	169.1(2)	0.2656(5)	0.2892(2)
800	169.5(2)	0.2677(6)	0.2899(2)
900	169.3(2)	0.2697(6)	0.2904(2)

phase at annealing temperatures above 1000°C. At these temperatures CLT phase was transformed into γ-Ti_3O_5 [30] and Ti_5O_9 phases [31]. The refinement, however, revealed that the crystallography of these phases was only a first approximation to the real crystalline structure of the new phases, because none of them fitted well to the experimental diffraction patterns. These new phases were not further analyzed in detail, because it was outside the scope of the present work.

As it was yet found for other nanocrystalline oxides [16,17,32], the atomic bond lengths and the symmetry of CLT phase depended on crystallite size (Tables 4, 6 and 7). The strongest change is observed for the Ti–O bonds, which corresponded to the atomic bond lengths T_1 and T_2: while T_1 decreased with crystallite size, T_2 increased. The angle between these bonds decreased from 172.7(1) to 169.3(2) degrees as the crystallite size increased (Table 7); the corresponding angle for Ti_2O_3 phase is 169.98(6)° [29]—in the octahedron derived from a cubic or a tetragonal crystalline structure this angle is 180.0°. This shows that the octahedron suffered a larger deformation as the crystallite size was increased, which obviously will affect the electronic properties of this phase. From an analysis of the atomic coordinates alone (Table 3 and 5) it is difficult to obtain the above conclusions, which shows the need and usefulness of giving the tables containing the atomic bond lengths.

It is interesting to note that brookite and anatase phases were stable even at 700°C (Table 1). The transformation of brookite into rutile occurred at 800°C, which is a relatively high temperature for this transformation, because it is normally observed at lower temperatures. For example, when brookite formation is induced by doping the sample with copper [33], at 800°C brookite transformation into rutile is total, or when the sample is prepared without doping, the transformation occurs at even lower temperatures [10].

The observed stability of brookite was probably also caused by hydroxyls strongly bounded to its crystalline structure during the hydrothermal treatment, hydroxyls that should be similar to those that hindered CLT crystallite growing. These hydroxyls could also cause the stability of anatase, which in the present case was transformed into rutile at annealing temperatures above 800°C. This high transformation temperature of anatase into rutile is only observed in sol–gel samples prepared with acetic acid as hydrolysis catalyst [10].

Although from the Rietveld analysis we obtained information for brookite, anatase and rutile, we are reporting in detail only the one corresponding to brookite, because this information is scarcely found in the literature, and it will be useful for modeling brookite's properties.

From the lattice parameters only a decreased as brookite's crystallite size increased (Tables 8); a similar behavior was observed for the y and z coordinates of titanium atom and for the z coordinate of the oxygen atoms in site O1 (Tables 8 and 9). The variation of these parameters changed the symmetry of the octahedron representative of this titanium polymorph (Fig. 6), and consequently the interaction between neighboring octahedra.

It is worthwhile to notice that the values of the crystallography parameters corresponding to the brookite observed after annealing the sample at 900°C did not follow the tendency observed when the sample was annealed at lower temperatures. Two causes could be responsible for this: First, the brookite concentration at

Table 8
Brookite lattice parameters and titanium atom coordinates as a function of sample annealing temperature

T (°C)	a (nm)	b (nm)	c (nm)	Ti_x	Ti_y	Ti_z
100	0.9175(3)	0.5455(1)	0.5139(1)	0.1301(6)	0.099(1)	0.8685(9)
200	0.9174(5)	0.5452(2)	0.5137(2)	0.129(1)	0.100(2)	0.868(2)
300	0.9174(4)	0.5454(2)	0.5136(2)	0.1291(8)	0.099(1)	0.867(1)
400	0.9166(4)	0.5451(2)	0.5133(2)	0.1295(8)	0.10(1)	0.866(1)
500	0.9169(4)	0.5455(2)	0.5134(2)	0.1290(8)	0.096(1)	0.866(1)
600	0.9164(5)	0.5454(3)	0.5132(2)	0.129(1)	0.095(2)	0.866(2)
700	0.9162(3)	0.5447(2)	0.5136(2)	0.129(1)	0.096(2)	0.865(2)
800	0.9165(6)	0.5448(3)	0.5136(2)	0.130(2)	0.094(3)	0.864(3)

Table 9
Brookite O1 and O2 atom coordinates as a function of sample annealing temperature

T (°C)	$O1_x$	$O1_y$	$O1_z$	$O2_x$	$O2_y$	$O2_z$
100	0.014(3)	0.143(4)	0.187(3)	0.238(1)	0.117(4)	0.529(1)
200	0.014(5)	0.16(1)	0.181(7)	0.244(2)	0.126(7)	0.525(5)
300	0.014(4)	0.146(6)	0.179(4)	0.241(2)	0.123(6)	0.531(4)
400	0.012(2)	0.142(4)	0.179(4)	0.235(2)	0.120(6)	0.530(4)
500	0.010(2)	0.142(6)	0.177(4)	0.236(4)	0.119(6)	0.525(4)
600	0.013(3)	0.143(5)	0.178(5)	0.234(8)	0.118(8)	0.530(5)
700	0.009(3)	0.148(5)	0.176(5)	0.231(8)	0.113(8)	0.527(5)
800	0.0157(6)	0.151(9)	0.175(9)	0.224(6)	0.11(1)	0.532(6)

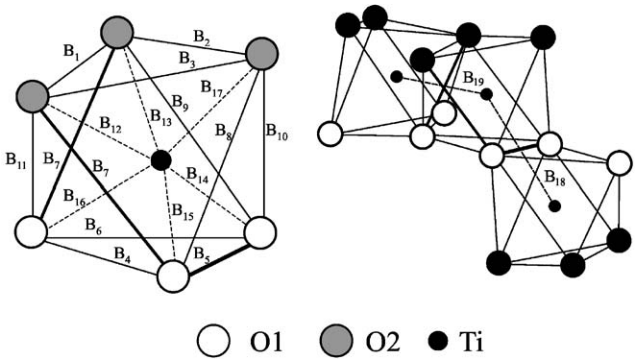

Fig. 6. Representative octahedron of brookite with the different atomic bond lengths associated to it. The B_5 and B_7 edges shared by neighboring octahedra are enhanced. The figure gives also details of how neighboring octahedra share their edges, and shows the two different Ti–Ti bonds, B_{18} and B_{19}, associated to this sharing.

this temperature was only 6(3) wt%, which produced high uncertainly in the corresponding parameters during the refinement. Second, the presence of the new titanium oxide phases obtained by the transformation of CLT phase at this temperature, which have a strong diffraction peak at the same position as the second strongest peak of brookite. This last situation will be the most important in affecting brookite's parameter, because the model for the crystalline structure of these phases was only a first approximation. Therefore, in the following analysis of brookite, the data corresponding to this temperature are discarded.

Table 10
Brookite some of the atomic bond lengths (in nm) associated to the representative octahedron as a function of sample annealing temperature

T (°C)	B_3	B_5	B_6	B_7	B_{18}	B_{19}
100	0.2736(1)	0.2489(1)	0.2815(1)	0.2568(1)	0.2946(1)	0.3055(1)
200	0.2728(2)	0.2454(2)	0.2828(2)	0.2579(2)	0.2945(2)	0.3046(2)
300	0.2733(2)	0.2446(2)	0.2835(2)	0.2542(2)	0.2945(2)	0.3051(1)
400	0.2739(2)	0.2413(2)	0.2830(2)	0.2539(2)	0.2935(2)	0.3067(1)
500	0.2740(1)	0.2395(1)	0.2835(1)	0.2570(2)	0.2931(2)	0.3066(1)
600	0.2743(2)	0.2414(2)	0.2835(2)	0.2525(3)	0.2929(3)	0.3071(2)
700	0.2745(2)	0.2428(2)	0.2832(2)	0.2533(3)	0.2933(3)	0.3069(2)
800	0.2765(2)	0.2435(2)	0.2836(2)	0.2479(3)	0.2952(3)	0.3080(2)

Brookite's crystallite size changed systematically with a well-defined tendency as the sample was annealed above 400°C. Some of the corresponding atomic bond lengths also changed above this temperature (Tables 10), showing that the local symmetry and the interaction between atoms depend on crystallite size, in a similar way as it was observed for CLT, rutile [16] and boehmite phases [17,32].

When the sample was annealed at 900°C, almost all the brookite and about 50% of the anatase were transformed into rutile. This is associated to a weakening in crescendo of the strong bond that maintains the polyhedra together, which corresponds to the atomic bond lengths B_5.

The crystalline structure of brookite is made of zigzag filaments of Ti–O octahedra along c-axis [6], which share the atomic bond length B_5 and the two bond lengths B_7. These filaments are connected between each other by the atoms associated to atomic bond lengths B_3 and B_6, producing sheets of octahedra parallel to b–c plane. These sheets are ordered along a-axis and bounded by the atomic bond length B_5 [6], which represents the strongest O–O interaction. The atomic bond lengths B_3 and B_6 increased as the annealing temperature increased (Table 10), showing a weakening of the respective bonds, which favored the transformation of brookite into rutile.

4. Conclusions

Titania samples rich in brookite were prepared under hydrothermal conditions by starting from $TiCl_3$ as titanium precursor. Samples also contained a new phase, named corundum-like titania, which in a first approximation has the same crystalline structure as Ti_2O_3, but in contrast to it, the new phase did not oxidize when it was annealed in air at high temperatures. To find the origin of its stability in air, it is necessary to prepare

samples with only this phase. The local symmetry and the atomic bond lengths of this phase and the ones of brookite depended on the crystallite size. From the evolution with temperature of the atomic bond lengths shared by contiguous octahedra forming the lattice, it was possible to predict the transformation of both phases during their annealing. The synthesis method described in the present work gave rise to brookite and anatase phases that were stable at very high temperatures; the origin of their stability, however, is unknown and requires the synthesis of single-phase samples to find it.

Acknowledgments

We would like to thank Mr. A. Morales and Eng. M. Aguilar for technical assistance. This work was partially financed with FIES D.00079; FIES-98-23-III project at the Instituto Mexicano del Petróleo, Mexico.

References

[1] G. Phani, G. Tulloch, D. Vittorio, I. Skryabin, Renewable Energy 22 (2001) 303.
[2] M. Najbar, J. Camra, Solid State Ionics 101–103 (1997) 707.
[3] S. Ono, Y. Nishi, S. Hirano, J. Am. Ceram. Soc. 84 (2001) 3054.
[4] A. Stoch, A. Brozek, G. Kmita, J. Stoch, W. Jastrzebski, A. Rakowska, J. Mol. Struct. 596 (2001) 191.
[5] J. Tang, S. Endo, J. Am. Ceram. Soc. 76 (1993) 796.
[6] X. Bokhimi, A. Morales, M. Aguilar, J.A. Toledo-Antonio, F. Pedraza, Int. J. Hydrogen Energy 26 (2001) 1279.
[7] H. Kominami, M. Kohno, Y. Kera, J. Mater. Chem. 10 (2000) 1151.
[8] P. Arnal, R.J.P. Corriu, D. Leclercq, P.H. Mutin, A. Vioux, J. Mater. Chem. 6 (1996) 1925.
[9] A. Pottier, C. Chanéac, E. Tronc, L. Mazerolles, J.-P. Jolivet, J. Mater. Chem. 11 (2001) 1116.
[10] X. Bokhimi, A. Morales, O. Novaro, T. López, E. Sánchez, R. Gómez, J. Mater. Res. 10 (1995) 2788.
[11] S. Yin, R. Li, Q. He, T. Sato, Mater. Chem. Phys. 75 (2002) 76.
[12] X. Bokhimi, A. Morales, O. Novaro, T. López, O. Chimal, M. Asomoza, R. Gómez, Chem. Mater. 9 (1997) 2616.
[13] A.K. Sharma, R.K. Thareja, U. Willer, W. Schade, Appl. Surf. Sci. 206 (2003) 137.
[14] T. Kuratomi, K. Yamaguchi, M. Yamawaki, T. Bak, J. Bowotny, M. Rekas, C.C. Sorrel, Solid State Ionics 154–155 (2002) 223.
[15] Y. Zheng, E. Shi, S. Cui, W. Li, X. Hu, J. Am. Ceram. Soc. 83 (2000) 2634.
[16] X. Bokhimi, A. Morales, F. Pedraza, J. Solid State Chem. 169 (2002) 176.
[17] X. Bokhimi, J.A. Toledo-Antonio, M.L. Guzmán-Castillo, B. Mar-Mar, F. Hernández-Beltrán, J. Navarrete, J. Solid State Chem. 161 (2001) 319.
[18] X. Bokhimi, J. Sánchez-Valente, F. Pedraza, J. Solid State Chem. 166 (2002) 182.
[19] S. Yamazaki, K. Hori, Catal. Lett. 59 (1999) 191.
[20] L. Pauling, J.H. Sturdivant, Z. Krystallogr. 68 (1928) 239.
[21] R. Weyl, Z. Krystallogr. 111 (1959) 401.
[22] I. Keesmann, Z. Anorg. Allg. Chem. 346 (1966) 30.
[23] J. Rodríguez-Carbajal, Laboratoire Leon Brillouin (CEA-CNRS), (France Tel: (33) 1 6908 3343, Fax: (33) 1 6908 8261, E-mail: juan@llb.saclay.cea.fr)
[24] P. Thompson, D.E. Cox, J.B. Hasting, J. Appl. Crystallogr. 20 (1987) 79.
[25] R.A. Young, P. Desai, Arch. Nauki Mater. 10 (1989) 71.
[26] D. Louër, T. Bataille, T. Roisnel, J. Rodriguez-Carbajal, Powder Diffraction 17 (2002) 262.
[27] J.-F. Bérar, P. Lelann, J. Appl. Crystallogr. 24 (1991) 1.
[28] E. Prince, J. Appl. Crystallogr. 14 (1981) 157.
[29] C.E. Rice, W.R. Robinson, Mater. Res. Bull. 11 (1976) 1355.
[30] S.-H. Hong, S. Åsbrink, Acta Crystallogr. B 38 (1982) 2570.
[31] S. Andersson, L. Jahnberg, Arkiv Kemi. 21 (1963) 413.
[32] X. Bokhimi, J.A. Toledo-Antonio, M.L. Guzmán-Castillo, F. Hernández-Beltrán, J. Solid State Chem. 159 (2001) 32.
[33] X. Bokhimi, A. Morales, O. Novaro, T. López, O. Chimal, M. Asomoza, R. Gómez, Chem. Mater. 9 (1997) 2616.